Highly crystalline zinc stannate nanocatalyst for rhodamine 6G degradation: synthesis and characterization

S. Haq[a,*], M. B. Ali[b], A. Mezni[c], A. Hedfi[b], W. Rehman[d], M. Waseem[e], F. U Rehman[d], B. Khan[d], S. U. Din[a], F. U. Rehman[a], S. A. Abbasi[a], A. L. Lone[a]
[a]*Department of Chemistry, University of Azad Jammu and Kashmir, Muzaffarabad 13100, Pakistan*
[b]*Department of Biology, College of Sciences, Taif University, P.O. Box 11099, Taif 21944, Saudi Arabia*
[c]*Department of Chemistry, College of Science, Taif University, P.O. Box 11099, Taif 21944, Saudi Arabia*
[d]*Department of Chemistry, Hazara University, Mansehra, Pakistan*
[e]*Department of Chemistry, COMSTAS University Islamabad, Islamabad, Pakistan*

The cubic shaped zinc stannate nanocatalyst (ZS-NC) with the average crystallite size of 32.58 nm was prepared by sol-gel method using ZnO and SnO_2 as a precursors. The crystal structural composition was investigated through Fourier transform infrared (FTIR) spectroscopy, X-ray diffraction (XRD) and energy dispersive X-ray (EDX). The microstructure analysis was done over scanning electron microscopy (SEM) and the optical property was studied by operating diffuse reflectance spectroscopy (DRS). The rhodamine 6G was degraded in aqueous under the influence of solar light in the presence of ZS-NC and photocatalytic parameters were derived by using a set of equations. It has been observed almost the dye (99.38%) was mineralized in 330 min with degradation rate of 1.281×10^{-2}/min.

(Received September 11, 2021; Accepted March 5, 2022)

Keywords: Zinc stannate, Nanocatalyst, Sol-gel, Mineralization, Conduction band

1. Introduction

In the last decades much interest have been paid to nanostructured of binary semiconducting metal oxides due to their unique applications [1]. An attention in ternary complex oxides has become noticeable for further improving their physical and chemical properties [2]. One of these semiconducting metal oxide is zinc stannate, which is a class of bimetallic oxide possess unique chemical and physical properties and are stable under extreme conditions [3]. Zinc stannate materials have versatile application in different fields including Li-Ion batteries, photo electrochemical cell, transparent conductive electrode and photocatalysts for the breakdown of organic dyes as it possess more photocatalytic action as compared to ZnO and SnO_2 [4–6]. Optical and electrical properties of tin oxide is effected by size and shape. So the control of size and shape is necessary. The ZS-NC is appropriate for a large no of applications in solar cells, for humidity recognition, negative electrode material for Li-ion batteries and a photocatalysts to remove organic impurities due to stability under extreme condition, attractive optical properties, high electrical conductivity and electron mobility [2,7]. Different approaches are used for the synthesis of ZS-NC nanocomposite including calcinations, thermal evaporation, sol-gel synthesis, mechanical grinding, hydrothermal synthesis, and ion-exchange methods [6–8]. Beside other methods, sol-gel method gained much attention due to its easy handling, low cost and better control over particle size [4,9]. Several study have been reported to investigate the photocatalytic activity of the ZS-NC against different harmful organic pollutants [4,7,9–11].

The present study was planned to synthesize ZS-NC by simple and low cost sol-gel method for the photodegradation of rhodamine 6G. The SEM, EDX, XRD, FTIR and DRS

* Corresponding author: siraj.ulhaq@ajku.edu.pk
https://doi.org/10.15251/JOR.2022.182.121

techniques were operated to investigate the structural and optical properties of ZS-NC. The photocatalytic activity was checked against rhodamine 6G under the solar light irradiation.

2. Experimental section

2.1. Materials used

The zinc oxide, tin dioxide, nitric acid, sodium hydroxide and ethanol was provided by Sigma-Aldrich and used without further purification. Deionized water was used throughout the research project.

2.2. Preparation of Zinc stannate nanocatalyst

ZS-NC is prepared by the reaction of zinc oxide and tin oxide in basic medium. For the synthesis of ZS-NC, zinc oxide and tin oxide (2:1) were dissolved in acidic solution of nitric acid individually. After complete. Both the solutions were than mixed with vigorous stirring at 70 °C and the pH was adjusted at 10 by dropwise addition of NaOH solution. After 4 hours the prepared gel was aged for 24 hours and then washing was done with hot distilled water twice followed by ethanol and drying is done in oven at 150 °C to obtain powdered sample.

2.3. Characterization

X-ray diffraction (XRD) measurement was carried out using a Panalytical X'pert pro (PW 3040/60) diffractometer in the two 2-theta range of 20° to 80°. The surface study of the prepared ZS-NC was examined with a carl-zeiss supra 40 field emission scanning electron microscope (FESEM) model JEOL 5910 (Japan). The percentage composition and purity of the synthesized nanoparticles was examined X-ray dispersive spectroscopy. The UV–Visible absorption was observed during the DRS analysis and band gap was determined through Tauc plot. Fourier-transform infrared (FTIR) measurement was carried out with a Shimadzu FTIR spectrophotometer model 8400S.

3.4. Photocatalytic activity

The photocatalytic experiment was performed by reacting ZS-NC and rhodamine 6G under the solar light in aqueous. For the photocatalytic degradation experiment, 50 mL of the rhodamine 6G (20 ppm) solution was stirred in dark in the presence of ZS-NC (30 mg) for 30 min and afterward the reaction was exposed to solar light (June, 11 am to 3 pm). After a constant interval of time (in min), 3 mL from the reaction was centrifuged and analyzed through spectrophotometer (Thermo Spectronic UV 500) to observed decrease in the λ-max with passage of time.

3. Results and Discussion

3.1. SEM analysis

The microstructual analysis was carrid out by SEM and the low and high magnifications micrographs are showsn in Fig. 3.1, shows polydisperse grains of ZS-NC. Beside some irregular shaped grains, most of the grains observed in both micrographs are nearly spherical shaped with visible boundries between them. In the high magnified image (Fig. 1(b)) the clear cracks are seen, suggest that the grains are formed by the aggriagtion of small size particles. The grains are seem to be composed of 15 to 30 small particles depending upon size of the grains. The grains size estimated from SEM image is ranging between 210 to 350 nm.

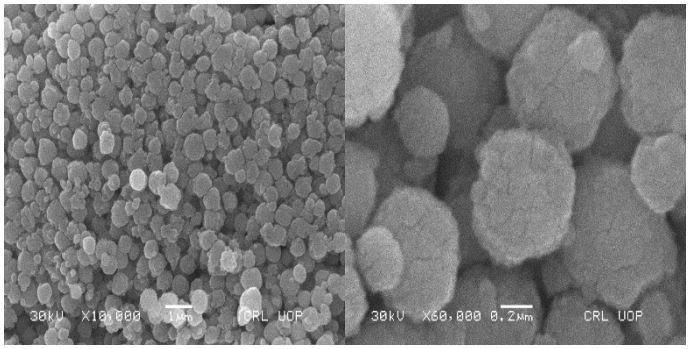

Fig. 1. Low and high magnified SEM micrographs of ZS-NC.

3.2. XRD analysis

Fig.2 illustrates the XRD pattern of ZS-NC, with the diffraction band at 2θ position with corresponding hkl values of 18.60 (111), 30.08 (220), 37.28 (222), 47.72 (331), 50.87 (411), 56.67 (511), 62.59 (531), 68.01 (620), 79.31 (551). These Bragg's reflections were found to be identical to the bands described in JCPDS card 00-024-1470, indicating that ZS-NC with cubic geometry was formed and the Fd3m space group. The sharp and intense bands suggest the well-crystalline nature of the ZS-NC with the avergae crystallite size of 34.28 nm and a lattice strain of 0.32 percent.

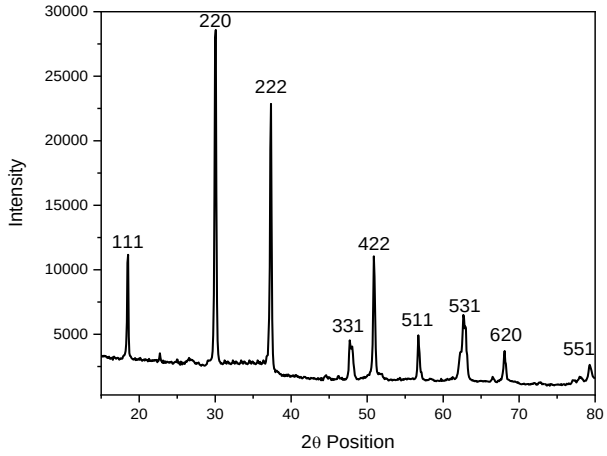

Fig. 2. XRD pattern of ZS-NC.

3.3. EDX analysis

The percentage composition and purity of ZS-NC are shown in the EDX spectrum in Fig. 3, showing the presence of Zn, Sn, and O. The presence of O can be seen in the signal at 0.4 keV, whereas Sn is responsible for the strong peak at 3.4 keV. Peaks at 1 keV and tiny bands at 8.7 and 9.6 keV indicate the presence of zinc. For Zn, Sn, and O, the weight percentages calculated from EDX data are 42.95, 36.33, and 20.71, respectively, which are extremely similar to theoretical values.

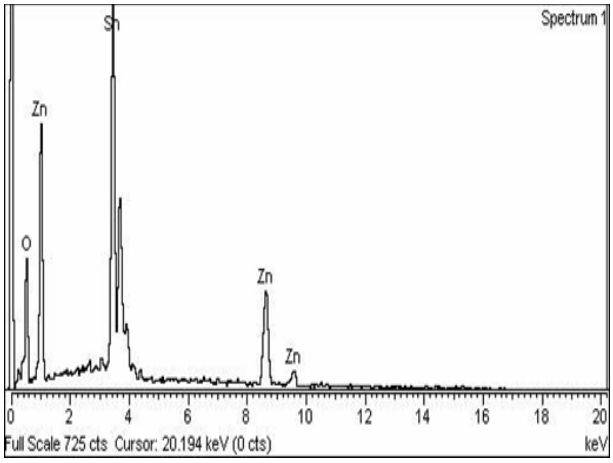

Fig. 3. EDX spectrum of ZS-NC.

3.4. DRS analysis

The varaition in the UV-Visible light transmittance phenomena was observed with increasing wave length in the region between 250-1000 nm as shwon in Fig. 4. With increasing wave length of light radiation, transmitance get increases suggest that maximum absorption occurred in the UV region [12]. The absorption of light lead to te optical transition of electron from valence band to conduction band and can be used to detemined the band gap by using Tauc plot [13]. The determied band gap energy is 3.12 eV, which is found smaller than that reported in literature [10,14].

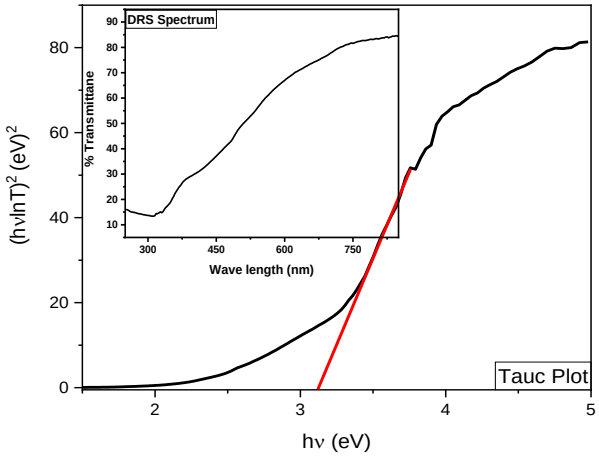

Fig. 4. Tauc plot (inset: DRS spectrum) of ZS-NC.

3.4. FTIR analysis

The presence of a hydroxyl group is confirmed by the band at 3485 and 1619 cm^{-1} in the FTIR spectrum of the ZS-NC as shown in Fig.5 [15]. The stretching vibration of O-Sn-O in the lattice structure causes the small band at 1017 cm^{-1} [16]. The peak at 897 and 709 cm^{-1} is due to Zn-O stretching vibrational groups, indicating possible Zn bonding in ZnO [17]. The transmittance peaks seen at 514 and 461 cm^{-1} are caused by stretching vibrations of ZnO and SnO_2 groups, and this might be attributed to Sn-O-Zn bonding in ZS-NC [18].

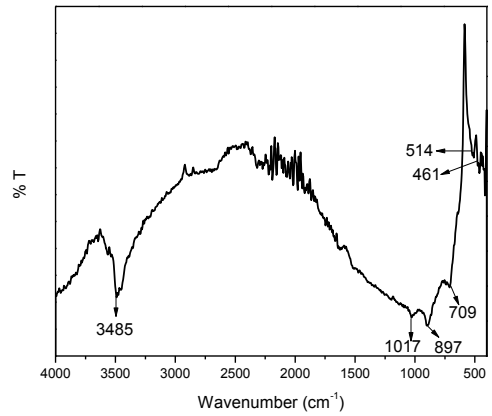

Fig. 4.7. FTIR spectrum of ZS-NC.

3.5. Photocatalytic analysis

The photocatalytic efficiency of the ZS-NC was checked against rhodamine 6G under solar light irradiation. The experiment was performed in the month June between 11 am to 3 pm. The Fig. 6(a) demonstrates the degradation of rhodamine 6G occurred by a progressive reduction in the absorbance maxima at 526 nm. Eq. 1 was used to determine the % degradation, where C_o and C_e are the beginning and final concentrations of rhodamine 6G, respectively [19,20]. The percentage degradation of rhodamine 6G in the presence of ZS-NC is 99.38 percent (Fig. 6(b)). The eq.2 was used to examine the photocatalytic reaction kinetics, where C_o and C_e are the beginning and final concentrations of rhodamine 6G, k and t are apparent constants [21]. A straight line plot with an r^2 value of 0.961 as shown in Fig. 6(c) implies that the photocatalytic process follows pseudo-first-order kinetics. According to the slope of linear plots, the photo-degradation rate constant for rhodamine 6G through ZS-NC is 1.281×10^{-2} min^{-1}.

$$\% \, Degradation = \frac{C_o - C_t}{C_o} \times 100 \qquad \text{(eq.1)}$$

$$\ln\left(C/C_o\right) = -kt \qquad \text{(eq.2)}$$

The electron excitation and hole creation mechanism is illustrated in Fig. 6(d). It shows that when light falls on the ZS-NC, the outermost electron is excited into the conduction band (CB), leaving a hole in the valence band (VB) [22]. The excited electrons gather in the CB of SnO_2, whereas the hole is transferred to the VB of ZnO [23]. The positive hole reacts with the water/hydroxyl group to form a hydroxyl radical while excited electrons combine with absorbed oxygen to generate superoxide radicals, which is an extra source for the production of hydroxyl radical [24]. The hydroxyl radical is a strong oxidizing agent that converts the rhodamine 6G into carbon dioxide and water [25].

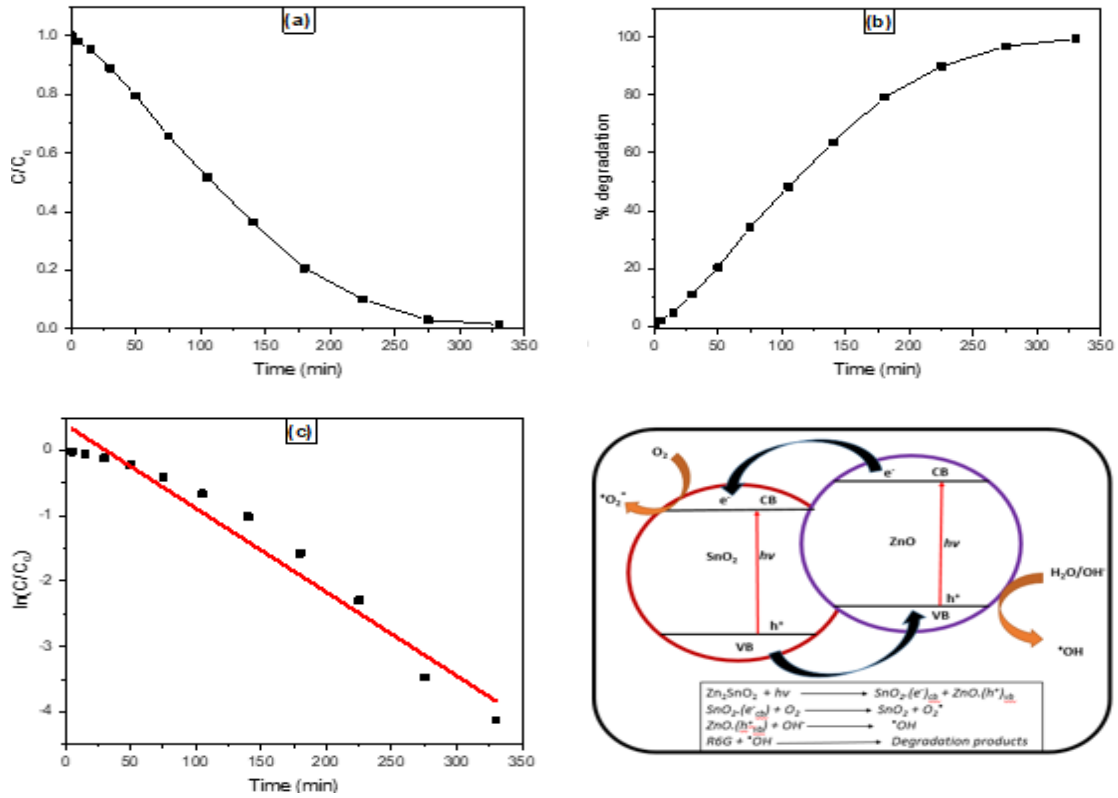

Fig. 6. Photocatalytic parameters like (a) = degradation profile; (b) = percentage degradation; (c) kinetic plot and electron excitation and hole creation mechanism.

4. Conclusions

The XRD analysis confirmed the formation of a stable and highly crystalline cubic ZS-NC by simple sol-gel method. The EDX analysis confirm the desired nanostructures are highly pure with no impurity. The band gap of ZS-NC was successfully reduced by the conjugation of SnO_2 and ZnO which play effective role in the degradation of process. Under the same reaction conditions, ZS-NC was found to be an effective photo-catalyst for the degradation of organic dye in aqueous medium.

Acknowledgments

The authors are grateful to the Deanship of Scientific Research for funding this article by Taif University Researchers Supporting Project number (TURSP-2020/28), Taif University, Taif, Saudi Arabia.

References

[1] H. Yuan, J. Xu, International Journal of Chemical Engineering and Applications 1, 241 (2010); https://doi.org/10.7763/IJCEA.2010.V1.41

[2] S. Baruah, J. Dutta, Science and Technology of Advanced Materials 12, (2011); https://doi.org/10.1088/1468-6996/12/1/013004

[3] L. A. Joseph, P. A. Vinosha, J. E. Jeronsia, M. M. Jaculine, S. J. Das, Journal of Taibah University for Science 10, 601 (2015); https://doi.org/10.1016/j.jtusci.2015.12.003

[4] B. Ayesha, U. Jabeen, A. Naeem, P. Kasi, M. Najam, K. Malghani, S. Ullah, J. Akhtar, M.

Aamir, Results in Chemistry 2, 100023 (2020); https://doi.org/10.1016/j.rechem.2020.100023

[5] S. Danwittayakul, M. Jaisai, T. Koottatep, J. Dutta, Industrial and Engineering Chemistry Research 52, 13629 (2013); https://doi.org/10.1021/ie4019726

[6] S. Sagadevan, J. Singh, K. Pal, Z. Zaman, Journal of Materials Science: Materials in Electronics 0, 0 (2017).

[7] M. H. Rasoulifard, M. S. S. Dorraji, S. Taherkhani, Journal of the Taiwan Institute of Chemical Engineers 58, 324 (2016); https://doi.org/10.1016/j.jtice.2015.06.008

[8] M. Miyauchi, Z. Liu, Z. G. Zhao, S. Anandan, K. Hara, Chemical Communications 46, 1529 (2010); https://doi.org/10.1039/b921010e

[9] N. Bibi, S. Haq, W. Rehman, M. Waseem, M. U. Rehman, A. Shah, B. Khan, P. Rasheed, Biointerface Research in Applied Chemistry 10, 5895 (2020).

[10] S. Shoukat, W. Rehman, S. Haq, M. Waseem, A. Shah, Materials Research Express 6, (2019); https://doi.org/10.1088/2053-1591/ab473c

[11] S. Dinesh, S. Barathan, V. K. Premkumar, G. Sivakumar, N. Anandan, Journal of Materials Science: Materials in Electronics (2016).

[12] S. Shoukat, S. Haq, W. Rehman, M. Waseem, M. Hafeez, S. U. Din, Zain-ul-Abdin, P. Ahmad, M. U. Rehman, A. Shah, B. Khan, Journal of Inorganic and Organometallic Polymers and Materials 31, 1565 (2021); https://doi.org/10.1007/s10904-020-01776-3

[13] P. Rasheed, S. Haq, M. Waseem, S. U. Rehman, W. Rehman, N. Bibi, S. A. A. Shah, Materials Research Express 7, (2020); https://doi.org/10.1088/2053-1591/ab6fa2

[14] M. H. Rasoulifard, M. S. S. Dorraji, S. Taherkhani, Journal of the Taiwan Institute of Chemical Engineers 000, 1 (2015).

[15] C. Wang, B. Q. Xu, X. Wang, J. Zhao, Journal of Solid State Chemistry 178, 3500 (2005); https://doi.org/10.1016/j.jssc.2005.09.005

[16] P. Kamaraj, R. Vennila, M. Arthanareeswari, S. Devikala, World Journal of Pharmacy and Pharmaceutical Sciences 3, 382 (2014).

[17] V. Kuzhalosai, B. Subash, A. Senthilraja, P. Dhatshanamurthi, M. Shanthi, Spectrochimica Acta - Part A: Molecular and Biomolecular Spectroscopy 115, 876 (2013); https://doi.org/10.1016/j.saa.2013.06.106

[18] K. Abdulkareem OMAR, B. Ismael Meena, S. Ali Muhammed, Physicochem. Probl. Miner. Process 52, 754 (2016).

[19] A. Shah, S. Haq, W. Rehman, W. Muhammad, S. Shoukat, M. ur Rehman, Materials Research Express 6, 045045 (2019); https://doi.org/10.1088/2053-1591/aafd42

[20] S. Haq, W. Rehman, M. Waseem, V. Meynen, S. U. Awan, A. R. Khan, S. Hussain, Zain-ul-Abdin, S. U. Din, M. Hafeez, N. Iqbal, Journal of Inorganic and Organometallic Polymers and Materials 31, 1312 (2021); https://doi.org/10.1007/s10904-020-01810-4

[21] S. Shoukat, W. Rehman, S. Haq, M. Waseem, A. Shah, Materials Research Express 6, 115052 (2019); https://doi.org/10.1088/2053-1591/ab473c

[22] E. Elhaddad, W. Rehman, M. Waseem, M. Nawaz, S. Haq, C. Y. Guo, Journal of Inorganic and Organometallic Polymers and Materials (2020).

[23] S. Haq, S. Shoukat, W. Rehman, M. Waseem, A. Shah, Journal of Molecular Liquids 318, 114260 (2020); https://doi.org/10.1016/j.molliq.2020.114260

[24] L. Qiu, Z. Zhou, Y. Yu, H. Zhang, Y. Qian, Y. Yang, S. Duo, Research on Chemical Intermediates 45, 1457 (2019); https://doi.org/10.1007/s11164-018-3675-7

[25] P. Van Viet, C. M. Thi, L. Van Hieu, Journal of Nanomaterials 1 (2016); https://doi.org/10.1155/2016/1957612